Electronic Supplementary Material (ESI) for ChemComm.

Supplementary Information

Thermally Responsive Reduced Graphene Oxide with Designable Secondary Functionality

Qian Zhang[a], Junhui Zhang[a], Bing Liu[a], Ling Zhang[b], Li Dong[a], Erni Li[a], Hairan Zhang[a], Lixin Xia[a*]

[a]*College of Chemistry, Liaoning University, Shenyang 110036, China*

[b]*College of Chemistry and Life Science, Shenyang Normal University, Shenyang 110034, China*

---

*Corresponding author. E-mail: lixinxia@lnu.edu.cn

**Corresponding authors. Tel: +86-24-62202258 (LXX); Fax: +86-24-62202258 (LXX)*

Experimental Details

1. Materials

Graphite powder with an average particle size of 325 meshes and a purity of over 99.9% was purchased from Alfa Aesar. 1-vinylimidazole (99%), bromoethane (98%) were purchased from Sigma-Aldrich and used as received. N-isopropylacrylamide (NIPAm) (99%) was purchased from J&K Scientific Ltd. and recrystallized from hexane/acetone. Azobisisobutyronitrile (AIBN) was purchased from Sigma-Aldrich and recrystallized from hexane. Potassium hexafluorophosphate (KPF_6), potassium ferricyanide (III) ($K_3[Fe(CN)_6]$), and sodium bisulfate ($NaHSO_4$) were purchased from Sinopharm Chemical Reagent Co. Ltd. (Shenyang, China) and used directly as received. All solutions were prepared using Milli-Q purified water (>18 MΩ cm^{-1}) sterilized at high temperature.

2. Apparatus and measurements

Transmission electron microscopy (TEM) was performed on a JEOL JEM-2100 electron microscope operating at 120 kV. The FTIR spectra were recorded on a Perkin Elmer Spectrum One instrument applying KBr pellets of the samples. Ultraviolet-visible (UV-vis) spectroscopic experiments were performed with Shimadzu UV-2100S spectrophotometer. X-ray photoelectron spectroscopy (XPS) were obtained using a LEO1530 field-emission SEM system and PHI1450 spectrometer. Atomic force microscopy (AFM) images were recorded with a Bruker Dimension icon atomic force microscopy. All samples for the AFM measurements were prepared by drop casting. Generally, 5 µl solution was dropped onto a freshly cleaved mica wafer with a diameter of 10 mm. Thermogravimetric analysis (TGA) was carried out using a SDTQ450 thermoanalyzer under nitrogen atmosphere at a heating rate of 10 °C min^{-1}. Raman spectra were obtained using a Renishaw inVia Raman microscope. A diode laser detected at 633 nm that the sample was illuminated through the microscope objective under normal incidence. Electrochemical measurements were carried out at room temperature using a BAS100B workstation. The measurements were based on a three-electrode system with the modified electrode as the working electrode, a Ag/AgCl electrode as the reference electrode, and a platinum wire as the counter electrode.

3. Synthesis of modified reduced graphene oxide (rGO)

3.1 Synthesis of graphene oxide (GO)

GO was prepared from graphite powder according to the modified Hummer method.[1] Firstly, graphite powder (2 g) and $NaNO_3$ (1.6 g) were put into 0 °C concentrated H_2SO_4 (67.5 mL) in a 250 mL flask. Then, $KMnO_4$ (9 g) was added gradually under vigorous stirring and the temperature of the mixture was kept to be lower than 20 °C by ice-bath. After the addition, the ice bath was removed, the reaction was maintained at 35 °C and the mixture was allowed to stir for 30 min. Deionized water (545 mL) was then gradually injected into the mixture followed by adding 30% H_2O_2 drop-wise until the solution became luminous yellow. For purification, the mixture was washed with 5% of HCl to remove metal ions followed by sufficient deionized water to remove the acid. Finally, the GO was obtained by filtrated the production and dried in vacuum for 24 h.

3.2 Synthesis of 1-vinyl-3-ethylimidazolium bromide

The ionic liquid monomer 1-vinyl-3-ethylimidazolium bromide (ViEtImBr) was synthesized according to the published literature.[2] 12.3 g (0.1 mol) of bromoethane were added drop-wise to 9.41 g (0.1 mol) of 1-vinylimidazole in a 100 mL reactor. The mixture was refluxed for 16 h. After cooling down, the resulting solid was washed several times with ethyl acetate. The white precipitate of ViEtImBr was then filtered and dried in a vacuum oven until constant weight.

3.3 Synthesis of poly(NIPAm-co-ViEtImBr)

It has been reported that functionalized copolymer could be formed via the copolymerization between ionic liquids monomer and other nonionic-ionic monomer.[3-4] According to this, the copolymer poly(NIPAm-*co*-ViEtImBr) was prepared via the free radical copolymerizations of NIPAm and ionic liquid monomer of ViEtImBr. NIPAm (3.96 g, 0.05 mol), ViEtImBr (1.01 g, 0.005 mol), AIBN (82 mg 0.5 mmol) and 50 mL of methanol were placed in a 100 mL flask with a magnetic stirring bar. The solution was sealed with a septum and degassed by bubbling with argon for 30 min. The reactor was then heated to 80 °C and kept stirring for 15 h. Successively, the reaction mixture was carefully added into 500 mL of diethyl ether drop by drop after the solutions was cooled to room temperature. The as formed white precipitate was separated out and then dried in vacuum for 12 h. Then, purification of the obtained polymer was performed by re-dissolving in methanol and exhaustively dialyzing against deionized water. Finally, the production of poly(NIPAm-*co*-ViEtImBr) was obtained by freeze-drying.

3.4 Synthesis of poly(NIPAm-co-ViEtImBr)-rGO

GO (45 mg) and deionized water (30 mL) were placed in a 100 mL flask, yielding an inhomogeneous yellow-brown dispersion. The yellow-brown dispersion was sonicated until it became clear with no visible particulate matter. Subsequently, copolymer poly(NIPAm-*co*-ViEtImBr) (1.2 g) was added into the dispersion. After the mixture was sonicated for another 30 min, hydrazine hydrate (0.6 mL) was added into the system. Then the flask was stirred in an oil bath thermostated at 100 °C for 24 h. The product was finally obtained after centrifugation and freeze-drying.

3.5 The reversible anion exchange reaction of poly(NIPAm-co-ViEtImBr)-rGO in aqueous solution

Poly(NIPAm-*co*-ViEtImBr)-rGO (0.1 g) was firstly dispersed in 10 mL of deionized water to form a stable black suspension. Subsequently, 1.2 equiv of KPF_6 with respect to imidazolium units of poly(NIPAm-*co*-ViEtImBr) was added to the uniform suspension. The anion exchange reaction between Br ion and PF_6 ion lead to a rapid and quantitative precipitation of rGO under aqueous conditions. The precipitation of rGO was then separated from the suspension via centrifugation. Afterwards, 10 mL of deionized water was re-added to the precipitation of rGO. Finally, upon the further addition of 1.5 equiv of KBr with respect to imidazolium units and stirring for 8 h, reversible anion exchange occurred and the uniform dispersion of hydrophilic rGO formed again.

3.6 Synthesis of multifunctionalized poly(NIPAm-co-ViEtIm[Fe(CN)$_6$)]-rGO and poly(NIPAm-co-ViEtIm[HSO$_4$])-rGO

Both of these two modified rGO were synthesized via the anion exchange reaction. In a typical procedure, a solution of $K_3[Fe(CN)_6]$ (0.15 g) in 3 mL of distilled water was added drop-wise to a solution of poly(NIPAm-*co*-ViEtImBr)-rGO (0.1 g) dispersed in 7 mL of distilled water. After 24 h of stirring at room temperature, the mixture was washed with hot deionized water for several times to remove the unmodified $Fe(CN)_6^{3-}$. The final poly(NIPAm-*co*-ViEtIm[Fe(CN)$_6$])-rGO was obtained after freeze-drying.

Similarly, poly(NIPAm-*co*-ViEtIm[HSO_4])-rGO was also been synthesized by the anion exchange reaction between $NaHSO_4$ and poly(NIPAm-*co*-ViEtImBr)-rGO.

To verify the actual replacement of Br ions with $Fe(CN)_6$ ions during the anion exchange process, an aqueous solution of pure $K_3[Fe(CN)_6]$ with a concentration of 0.2 mM was firstly configured. It is obvious that there was no other anions existed in such solution except $Fe(CN)_6^-$. Subsequently, the excessive poly(NIPAm-*co*-ViEtImBr)-rGO of 0.78 g was added to the $K_3[Fe(CN)_6]$ solution. The formed suspension was further stirred overnight to achieve the anion exchange reaction. Afterwards, the modified rGO was separated via centrifugation to obtain a clear supernatant. Finally, aqueous solution of $AgNO_3$ was added into the supernatant. It can be observed that a pale yellow precipitate formed quickly after the addition of $AgNO_3$ solution. The structure of precipitation was confirmed by the characterization of XRD. Uv-vis spectroscopy was utilized to monitor the anion exchange process.

4. Fabrication of various rGO electrodes

Prior to use, glassy carbon (GC) electrodes with a diameter of 3 mm were polished on a polishing cloth with 1.0, 0.3, 0.05 μm alumina powder respectively and rinsed with deionized water followed by sonicating in acetone, ethanol and deionized water successively. The electrodes were then dried with a purified nitrogen stream.

poly(NIPAm-*co*-ViEtIm[$Fe(CN)_6$])-rGO/GC electrodes were prepared by a simple casting method. Firstly, 7 μL poly(NIPAm-*co*-ViEtIm[$Fe(CN)_6$])-rGO aqueous dispersion was cast onto the GC electrode. Thereupon a beaker was covered over the electrode so that water could evaporate slowly in air and a uniform film electrode formed. For comparison, poly(NIPAm-*co*-ViEtImBr)/GC and poly(NIPAm-*co*-ViEtImBr)-rGO/GC electrodes were prepared with the same procedures as described above.

1. W. S. Hummers and R. E. Offeman, *J. Am. Chem. Soc.*, 1958, **80**, 1339-1339.
2. R. Marcilla, J. A. Blazquez, J. Rodriguez, J. A. Pomposo and D. Mecerreyes, *J. Polym. Sci. Part A: Polym. Chem.*, 2003, **42**, 208-212.
3. H. Chen, J.-H. Choi, D. Salas-de la Cruz, K. I. Winey and Y. A. Elabd, *Macromolecules*, 2009, **42**, 4809-4816.
4. D. Mecerreyes, *Prog. Polym. Sci.*, 2011, **36**, 1629-1648.

Supplementary Data

Synthetic route and characterization of copolymer poly(NIPAm-co-ViEtImBr)

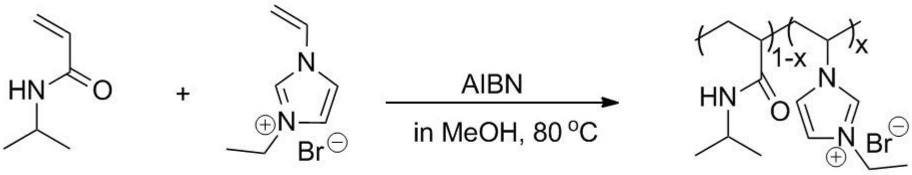

Fig. S1 Synthetic route to copolymer poly(NIPAm-*co*-ViEtImBr).

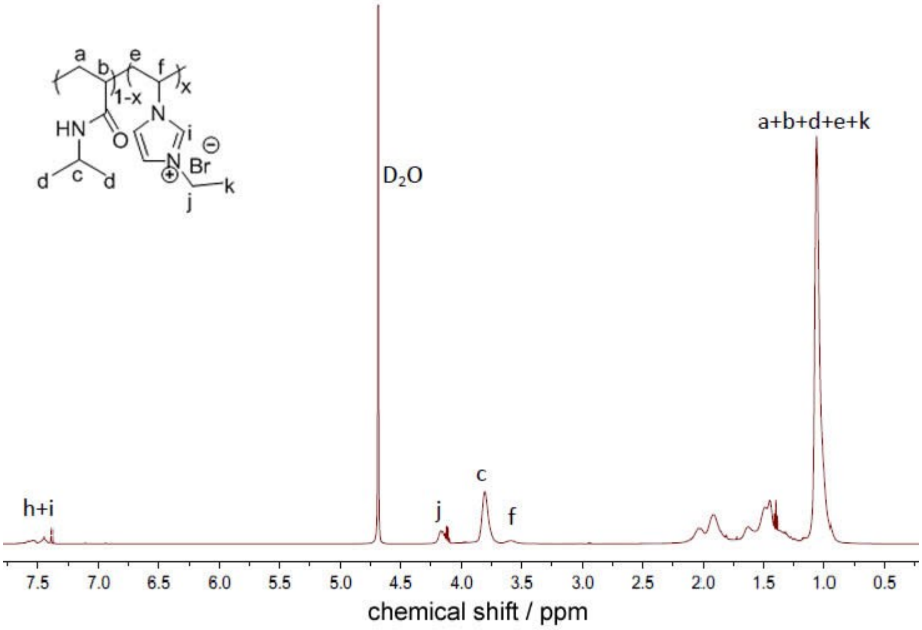

Fig. S2. ^{1}H-NMR spectra of poly(NIPAm-*co*-ViEtImBr) in D_2O.

Characterization of GO and poly(NIPAm-co-ViEtImBr)-rGO

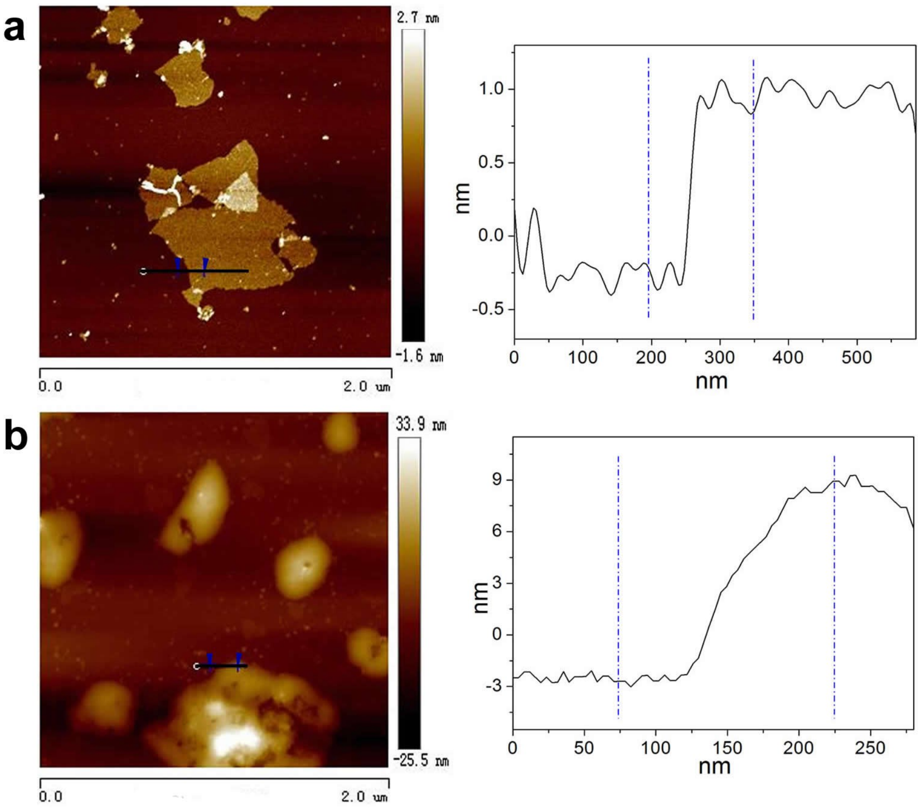

Fig. S3 Tapping mode AFM images and corresponding height profiles of GO (a) and poly(NIPAm-*co*-ViEtImBr)-rGO (b).

The tapping mode AFM images and corresponding height profiles of GO and poly(NIPAm-*co*-ViEtImBr)-rGO are shown in Figure S3. From the height profile, the thickness of GO sheets was found to be 1.05 nm, clearly suggesting almost a complete exfoliation of GO sheets. In contrast, on polymerization with poly(NIPAm-*co*-ViEtImBr), the thickness of poly(NIPAm-*co*-ViEtImBr)-rGO increased to 10.8 nm, indicating that the poly(NIPAm-*co*-ViEtImBr) chains were successfully grafted from the surfaces of rGO sheets. The thickness of the modified poly(NIPAm-*co*-ViEtImBr) was estimated to be around 9 nm.

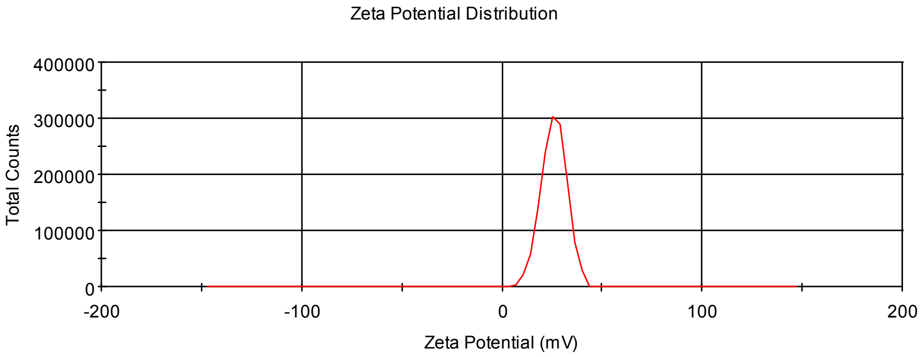

Fig. S4. The Zeta potential data of poly(NIPAm-*co*-ViEtImBr)-rGO in aqueous solution at room temperature.

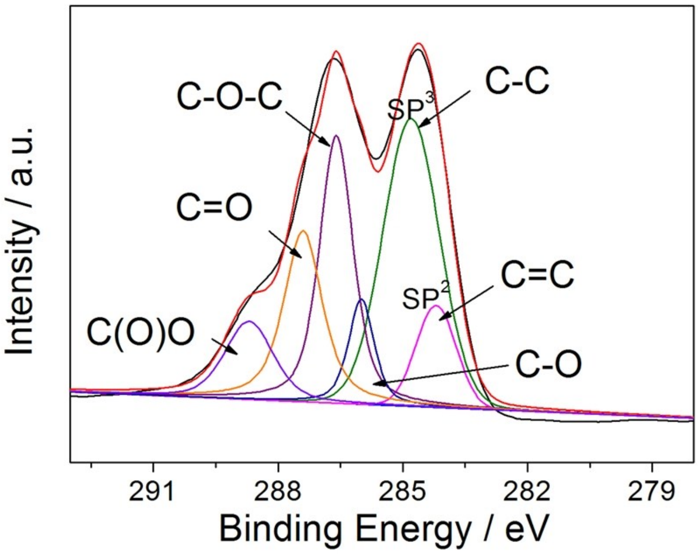

Fig. S5. C 1s core level spectra of GO.

Figure S5 shows the C 1s core level spectra of GO. As shown, the C 1s XPS peaks of GO were curve-fitted into the following components, which are sp^2 carbon C=C and sp^3 carbon C-C in aromatic rings, oxygenated carbon including hydroxyl carbon C-O, epoxy carbon C-O-C, carbonyl carbon C=O and carboxyl carbon C(O)O. The considerable degree of oxidation with six different carbon environments located at 284.2, 284.8, 286.0, 286.6, 287.4 and 289.4 eV, respectively. The percentage of sp^2 C and sp^3 C of GO was estimated to be 8.5% and 34.5% respectively.

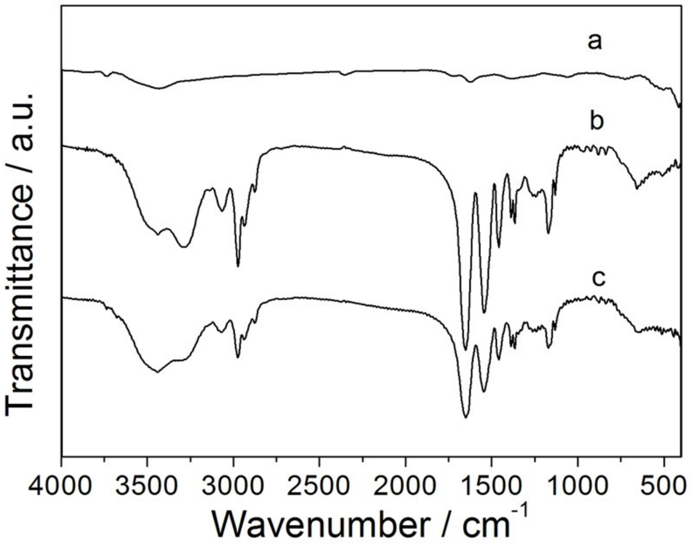

Fig. S6 FT-IR spectra of GO (a), poly(NIPAm-*co*-ViEtImBr) (b), and poly(NIPAm-*co*-ViEtImBr)-rGO (c).

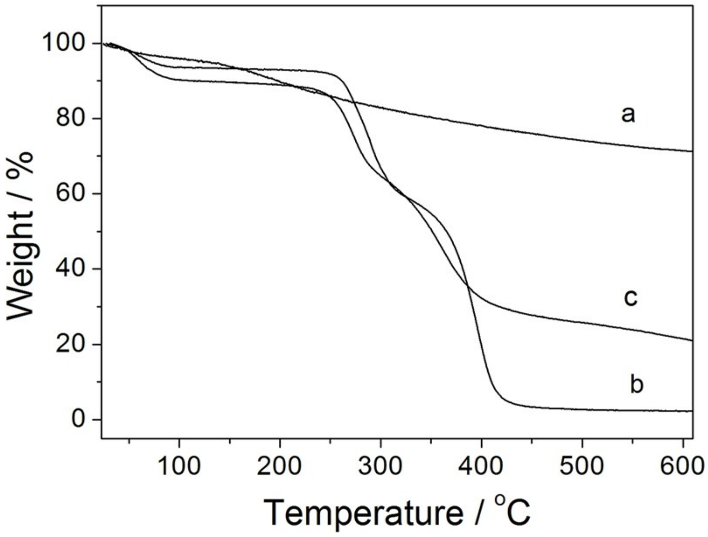

Fig. S7. TGA traces of GO (a), poly(NIPAm-*co*-ViEtImBr) (b), and poly(NIPAm-*co*-ViEtImBr)-rGO (c), measured under nitrogen and a heating rate of 10 °C/min.

Stimuli-responsive behaviour of various graphene materials

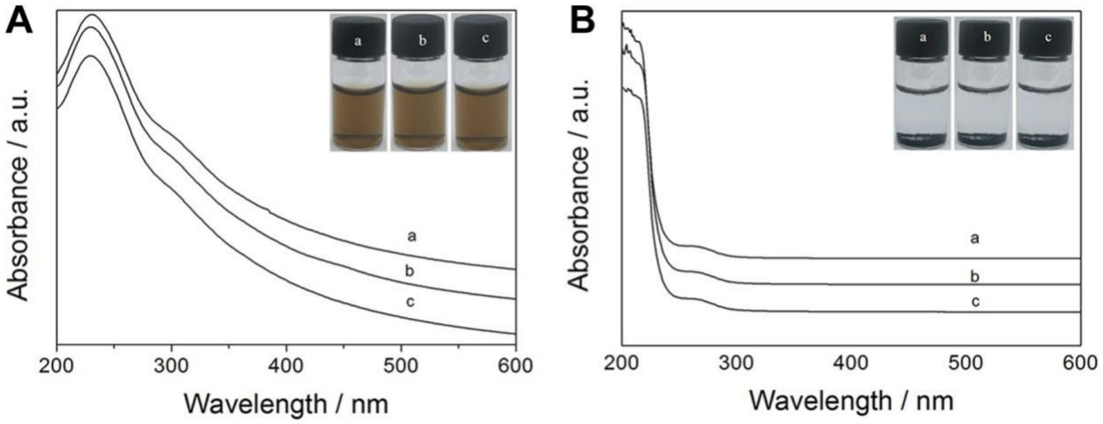

Fig. S8 UV-vis absorption spectra of aqueous solutions of GO (A) and rGO without modification (B) monitored at 20 °C (a), 45 °C (b) and recovering back to 20 °C (c) respectively, demonstrating no thermal responsiveness was observed at these two aqueous dispersions of nanosheets. Inset is the relevant photographs of various dispersion.

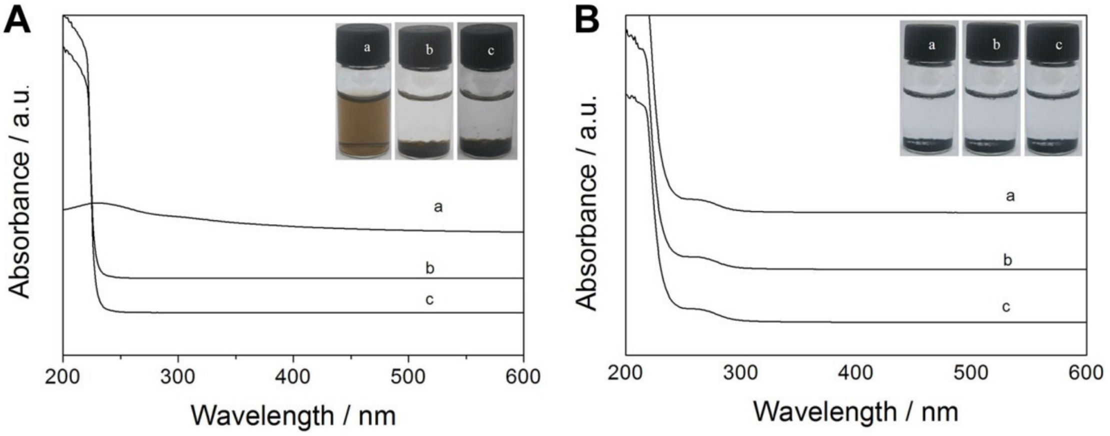

Fig. S9 UV-vis absorption spectra of aqueous solution of GO (A) and rGO without modification (B) monitored at original state (a), state of with the addition of KPF_6 (b) and state of with further addition of excess KBr after removing of previous KPF_6 (c). Inset is the relevant photographs of various dispersions of nanosheets during the process of adding KBr and KPF_6.

The unchanged states of precipitates after the addition of different kind of anions clearly demonstrated that no reversible anionic responsiveness was exhibited at these two aqueous solutions of nanosheets.

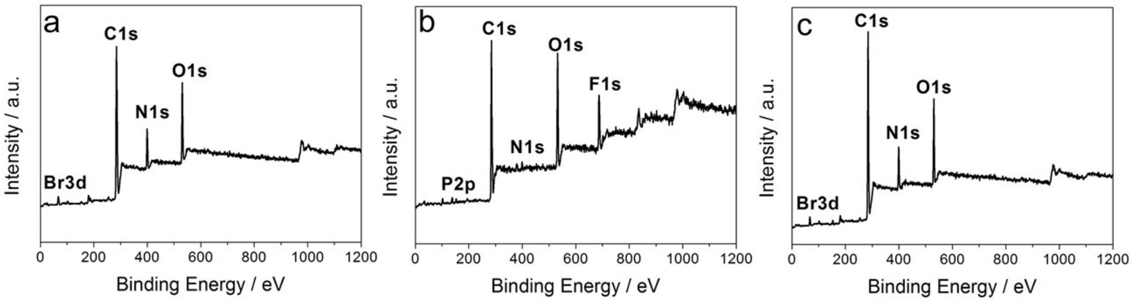

Fig. S10 XPS wide-scan spectra of poly(NIPAm-*co*-ViEtImBr)-rGO (a), poly(NIPAm-*co*-ViEtIm[PF$_6$])-rGO (b) and poly(NIPAm-*co*-ViEtImBr)-rGO obtained after anion exchange reaction between poly(NIPAm-*co*-ViEtIm[PF$_6$])-rGO and KBr (c).

According to the wide scan XPS spectra displayed in Fig. S10, it can be found that the P 2p and F 1s signal at binding energies about 138.3 eV and 687.5 eV in spectra of poly(NIPAm-*co*-ViEtIm[PF$_6$])-rGO were significantly. The existence of P and F elements in poly(NIPAm-*co*-ViEtIm[PF$_6$])-rGO is likely due to the introduction of PF$_6^-$ by exchanging the anions of PIL units. However, these characteristic peaks disappeared at the curve of the poly(NIPAm-*co*-ViEtImBr)-rGO after poly(NIPAm-*co*-ViEtIm[PF$_6$])-rGO further anion exchanged with excess KBr. On the basis of such variation of wide scan XPS spectra, it can be confirmed that the anion responsive behavior of poly(NIPAm-*co*-ViEtImBr)-rGO in aqueous solution was originated from the anion exchange property of PIL units in modified copolymer.

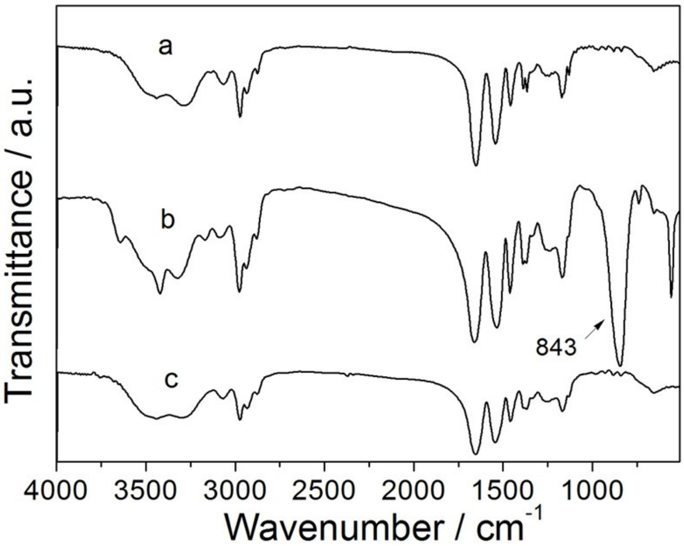

Fig. S11 FT-IR spectra of poly(NIPAm-*co*-ViEtImBr)-rGO (a), poly(NIPAm-*co*-ViEtIm[PF_6])-rGO (b) and poly(NIPAm-*co*-ViEtImBr)-rGO obtained after poly(NIPAm-*co*-ViEtIm[PF_6])-rGO further anion exchanged with excess KBr (c).

Figure S11 shows the FTIR spectra monitored during the anion responsive process of poly(NIPAm-*co*-ViEtImBr)-rGO in aqueous solution. After the first anion exchange process of replacing halide with PF_6^-, adsorption bands of PF_6^- at 843 cm^{-1} appeared in the FTIR spectrum of poly(NIPAm-*co*-ViEtIm[PF_6])-rGO. Upon the further anion exchange reaction between poly(NIPAm-*co*-ViEtIm[PF_6])-rGO and excess KBr, it can be observed that such characteristic band of PF_6^- disappeared in curve c, indicating that the paired anion of PF_6^- in PIL units has been completely replaced back to Br^-.

Characterization of functionalized thermal responsive rGO

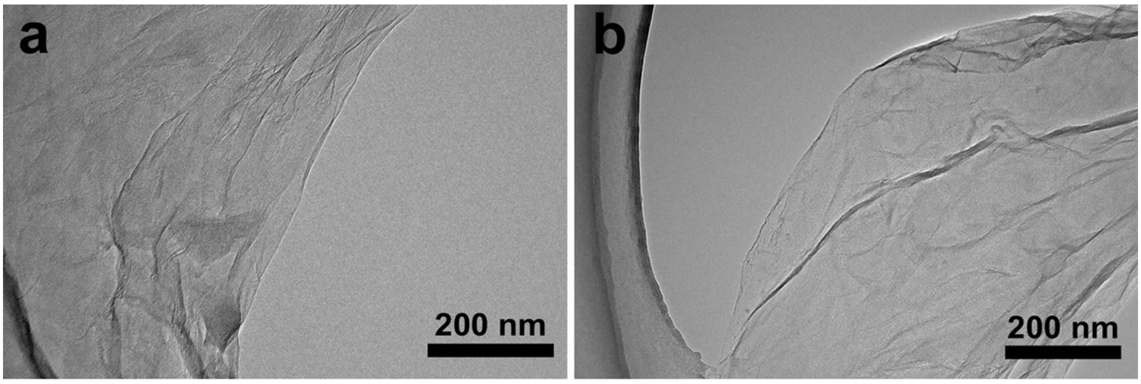

Fig. S12 TEM images of poly(NIPAm-*co*-ViEtIm[Fe(CN)$_6$])-rGO (a) and poly(NIPAm-*co*-ViEtIm[HSO$_4$])-rGO (b). The TEM images demonstrated that the functionalized rGO well preserved their original sheet-like morphologies.

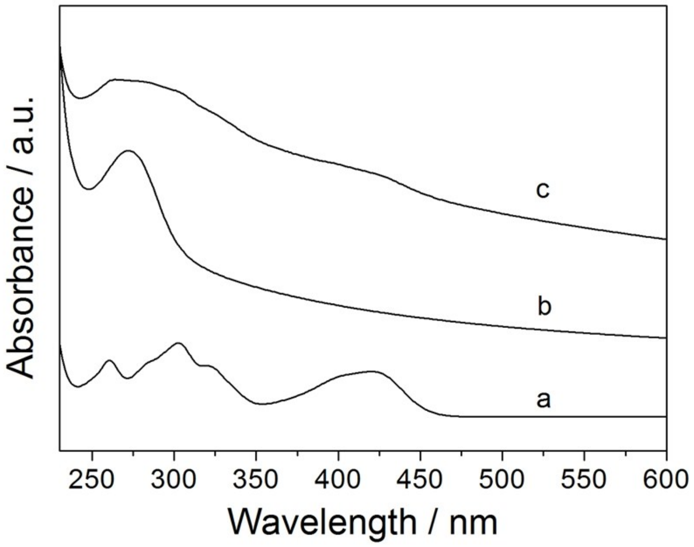

Fig. S13 UV-vis absorption spectra of $K_3Fe(CN)_6$ (a), poly(NIPAm-*co*-ViEtImBr)-rGO (b) and poly(NIPAm-*co*-ViEtIm[Fe(CN)$_6$])-rGO (c) in aqueous solution.

The characteristic peaks of $K_3Fe(CN)_6$ located at 302 and 423 nm (curve a) can be observed in the spectrum of poly(NIPAm-*co*-ViEtIm[Fe(CN)$_6$])-rGO dispersion (curve c) after the anion exchange reaction occurred between poly(NIPAm-*co*-ViEtImBr)-rGO and $K_3Fe(CN)_6$, demonstrating the modification of redox anion $Fe(CN)_6^{3-}$ on thermal responsive rGO.

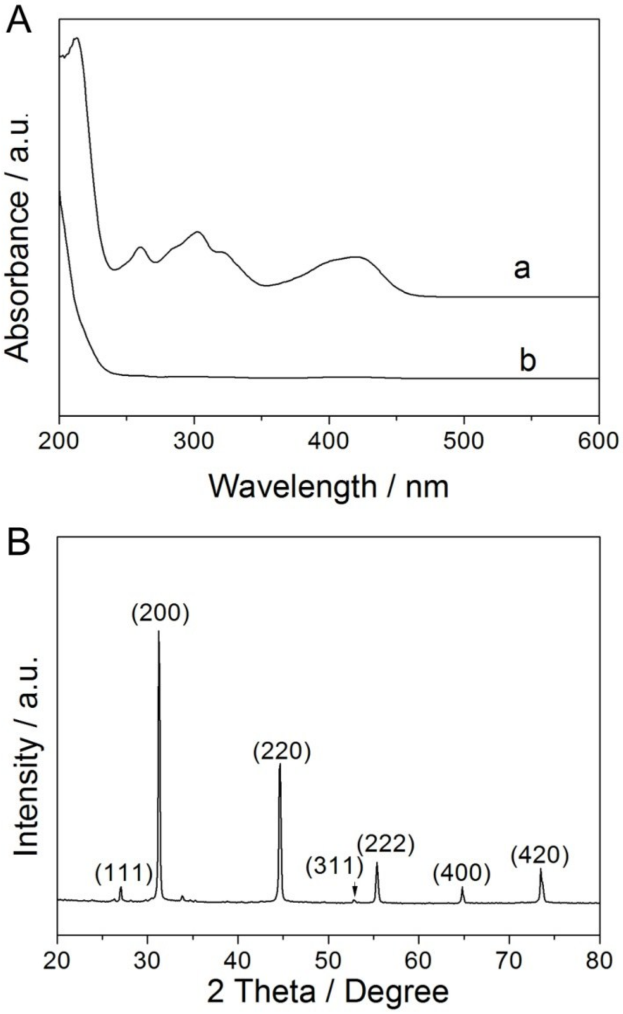

Fig. S14 Uv-vis spectra of $K_3[Fe(CN)_6]$ solution before (a) and after (b) the anion exchange reaction with poly(NIPAm-*co*-ViEtImBr)-rGO. (B) XRD pattern of the pale yellow precipitate obtained after the addition of $AgNO_3$ solution to supernatant.

Uv-vis spectroscopy was utilized to monitor the process of anion exchange reaction. It can be observed in curve a of Fig. S14A that the original solution of $K_3[Fe(CN)_6]$ exhibited obvious characteristic peak of anion $Fe(CN)_6^{3-}$ located at 421 nm. However, it could be observed that such characteristic peak completely disappeared in curve b after the reaction between $K_3[Fe(CN)_6]$ and poly(NIPAm-*co*-ViEtImBr)-rGO, indicating the removal of $Fe(CN)_6$ ion in supernatant. Meanwhile, after such supernatant was treated with $AgNO_3$ solution, a pale yellow precipitate could be obtained. The XRD pattern of the pale yellow precipitate was shown in Fig. S14B. As shown, the 2θ values at 26.7°, 31.0°, 44.3°, 52.5°, 55.0°, 64.5° and 73.2° corresponded to the (111), (200), (220), (311), (222), (400) and (420) crystal planes of cubic phase AgBr (JCPDS card no. 06-0438), indicating the transition of $AgNO_3$ to

AgBr occurred in the supernatant. It should be noticed that no Br ion was added to the solution during the whole process. The only complex involving in the process that having component of Br ion in its structure was poly(NIPAm-*co*-ViEtImBr)-rGO. So, it can then be deduced that the anion exchange reaction between modified rGO and $K_3[Fe(CN)_6]$ do occurred as expected.

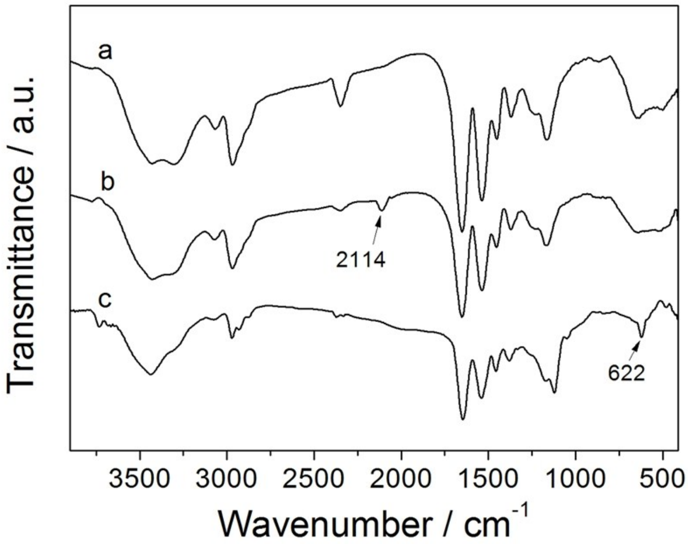

Fig. S15 FT-IR spectra of poly(NIPAm-*co*-ViEtImBr)-rGO (a), poly(NIPAm-*co*-ViEtIm[$Fe(CN)_6$])-rGO (b) and poly(NIPAm-*co*-ViEtIm[HSO_4])-rGO (c).

The characteristic bands of $Fe(CN)_6^{3-}$ and HSO_4^- appeared at 2114 and 622 cm^{-1} (curve b and c) respectively can be well observed in the corresponding spectra of poly(NIPAm-*co*-ViEtIm[$Fe(CN)_6$])-rGO and poly(NIPAm-*co*-ViEtIm[HSO_4])-rGO after anion exchange reaction, indicating the successful modification of function anions on thermal responsive rGO.

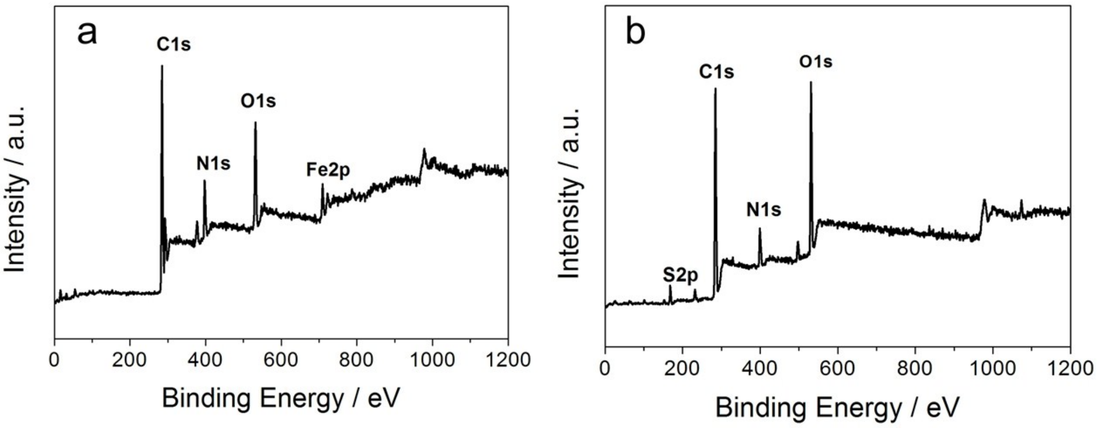

Fig. S16 XPS wide-scan spectra of poly(NIPAm-*co*-ViEtIm[Fe(CN)$_6$])-rGO (a) and poly(NIPAm-*co*-ViEtIm[HSO$_4$])-rGO.

From the wide scan XPS spectra, the Fe 2p signal at binding energies about 720 eV and the S 2p signal at binding energies about 180 eV can be observed significantly. Therefore, it can be confirmed that poly(NIPAm-*co*-ViEtIm[Fe(CN)$_6$])-rGO and poly(NIPAm-*co*-ViEtIm[HSO$_4$])-rGO were synthesized successfully by anion exchange reaction.

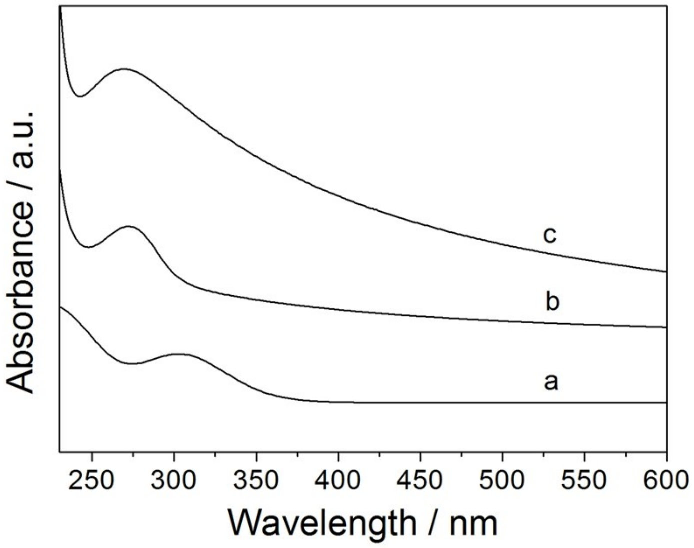

Fig. S17 UV-vis absorption spectra of NaHSO$_4$ (a), poly(NIPAm-*co*-ViEtImBr)-rGO (b), poly(NIPAm-*co*-ViEtIm[HSO$_4$])-rGO (c) in aqueous solution.

It can be observed that the characteristic peak of poly(NIPAm-*co*-ViEtIm[HSO_4])-rGO is broader than that of appeared in spectrum of poly(NIPAm-*co*-ViEtImBr)-rGO, which is due to the overlap of the peaks of HSO_4^- at 307 nm (curve a) and the characteristic band of poly(NIPAm-*co*-ViEtImBr)-rGO at 270 nm (curve b). Such result indicates the successful modification of acidic anion HSO_4^- on rGO via anion exchange reaction.

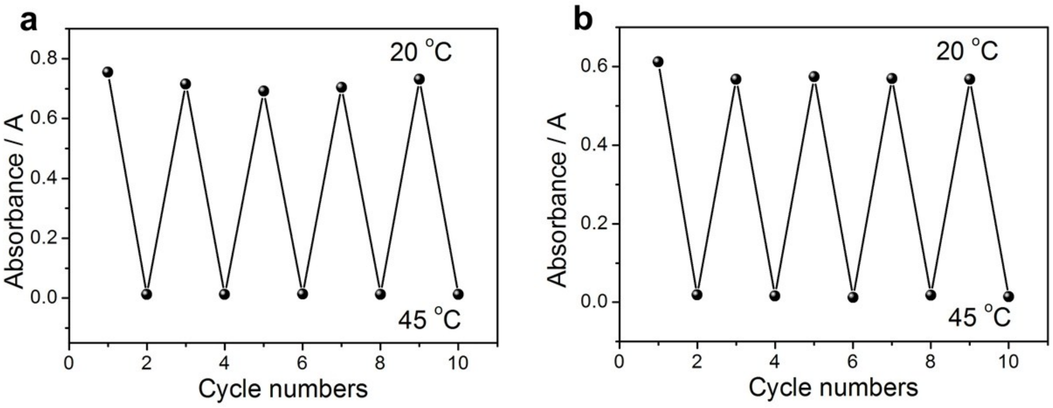

Fig. S18 The changes of intensity of UV-vis absorption peak at 280 nm of poly(NIPAm-*co*-ViEtIm[$Fe(CN)_6$])-rGO (a) upon temperature variation. The changes of intensity of UV-vis absorption peak at 275 nm of poly(NIPAm-*co*-ViEtIm[HSO_4])-rGO (b) upon temperature variation.

Similar to that of poly(NIPAm-*co*-ViEtImBr)-rGO, the changes of intensity of UV-vis absorption peaks at 280 nm and 275 nm show that both of poly(NIPAm-*co*-ViEtIm[$Fe(CN)_6$])-rGO and poly(NIPAm-*co*-ViEtIm[HSO_4])-rGO well displayed reversible and reproducible switching between hydrophilic to hydrophobic state in aqueous solution when the temperature varied between 20 °C and 45 °C.